

Numerical Research on Liquid Spray in Supersonic Cross Flow

Lianjie Yue¹, Gong Yu²

Institute of Mechanics, Chinese Academy Sciences¹
Email: yuelj@hotmail.com

Abstract

Numerical simulation was conducted to study the kerosene spray characteristics injecting into supersonic cross flow. The verification of the simulation was carried out by experimental Schlieren image, and the agreement was obtained by compared the spray plume pictures. Furthermore, the aerodynamic secondary breakup effect of the supersonic cross flow on the initial droplets was investigated. It was revealed that the initial parent drops were broken up into small drops whose diameter is about O(10) micrometers soon after they entered into the supersonic cross flow. During the appropriate range of initial drop size, the parent droplets would be broken up into small drops with the same magnitude diameter: no matter how large the initial drops SMD was.

Key Words: Liquid Spray, Two-Phase Flow, Supersonic Flow, Numerical Simulation

1. Introduction

As compared to hydrogen, liquid hydrocarbons, such as kerosene, are attractive candidates for fueling the scramjet in the lower hypersonic flight regime of $M < 8$ due to their significant benefits in terms of energy density and handling issues^[1]. However, up to now, the complex spray phenomena can't be understood well due to the limit of experimental measurement technique. Additionally, numerical simulations were seldom found in the literatures.

A modified code was developed by the author based on KIVA-3 to simulate liquid spray in supersonic flow^[2]. KIVA is a code written for internal combustion engine by the Los Alamos National Laboratory, which can analyze transient, three-dimensional, multiphase, and multi-component flow including chemically reaction with spray^[3]. Although spray models, the boundary conditions, special specifications and mesh generation are designed for IC engine, its equations and solution procedure possess generality, and the range of validity of the code can extend from low speeds to supersonic flows with laminar and turbulent regimes. So some necessary modifications can be made to simulate the spray in supersonic flow.

The kerosene spray in supersonic cross flow was elementarily calculated using the modified code^[2]. It was found that the penetration of the kerosene jet into the supersonic cross flow increase with the orifice diameter and the momentum ratio of the jet to the cross flow. Furthermore, there was strong interaction between the airflow and the kerosene spray. The gas velocity downstream of the injector dramatically decelerates due to the impact of the spray on the gas flow. And a clear streamwise vortex is formed due to the upward moving of the kerosene jet. Meanwhile, initial parent drops are broken up into small drops soon after they enter the supersonic cross flow.

The objective of present research is to further study

spray characteristics and the secondary breakup effect of the supersonic cross flow on the initial droplets.

2. Numerical Models and Methods

A stochastic particle method is used to calculate the liquid sprays, in which transport of the dispersed phase is calculated by tracking the trajectories of a certain number of representative parcels. Various sub-models account for the effects of turbulent dispersion, droplet collisions, evaporation and aerodynamic breakup. The mass, momentum, and energy exchange between the spray and the gas is also taken into account by adding source terms into the gas equations.

Turbulence Model

In order to account for the effects of compressibility, RNG $k-\varepsilon$ model was used, and a new term S_R was introduced in the ε equation of standard $k-\varepsilon$ turbulence model.

$$S_R = -\frac{c_\mu \eta^3 (1 - \eta/\eta_0)}{1 + \beta \eta^3} \rho \frac{\varepsilon^2}{k} \quad (1)$$

$$\eta = S \frac{k}{\varepsilon}$$

$$S = (2s_y s_{ij})^2$$

Where, $\eta_0 = 4.38$, $\beta = 0.012$, original model constants were also changed slightly, see Ref (4).

Motion of Droplets

The effect of aerodynamic drag and gravitational force on droplet acceleration was considered, as shown in Eq.(2).

$$\frac{d\bar{v}_p}{dt} = \frac{3}{8} \frac{\rho}{\rho_d} \frac{|\bar{u} + \bar{u}' - \bar{v}_p|}{r} (\bar{u} + \bar{u}' - \bar{v}_p) C_D + \bar{g} \quad (2)$$

TAB Breakup Model

The TAB breakup model considers a liquid drop to be analogous to a spring-mass system (Taylor's analogy). The external force is supplied by the gas aerodynamic forces on the droplet. The restoring force is supplied by the surface tension forces. Damping is supplied by liquid viscosity^[5]. The oscillation of the drop surface is described by a second order ordinary differential equation:

$$\ddot{y} = \frac{2}{3} \frac{\rho}{\rho_d} \frac{(\bar{u} + \bar{u}' - \bar{v}_p)^2}{r^2} - \frac{8\sigma}{\rho_d r^3} y - \frac{5\mu_l}{\rho_d r^2} \dot{y} \quad (3)$$

In which, y is proportional to the displacement of the equator of the droplet from its equilibrium position, divided by half droplet radius. The drop breakup is due to an increase in the amplitude of the drop oscillation. Breakup occur if and only if $y \geq 1$.

Turbulent Dispersion of Droplets

The dispersion of droplets due to gas phase turbulence is modeled by adding to the gas velocity a fluctuating velocity \bar{u}' , each component \bar{u}' follows a Gaussian distribution with mean square deviation $2/3 k$,

$$G(\bar{u}') = (4/3 \pi k)^{-1/2} \exp\left\{-3\bar{u}'^2/4k\right\} \quad (4)$$

The sampled fluctuating velocity is applied over the turbulence correlation time, which is the minimum of the eddy breakup time and a time for the droplet to traverse the eddy.

Droplet Evaporation

The rate of droplet radius change is given by the Frossling correction

$$\frac{dr}{dt} = - \frac{(\rho D)_{air} \left(\frac{\bar{T}}{T}\right) Y_1^* - Y_1}{2\rho_d r} Sh_d \quad (5)$$

The temperature of the droplet can be determined by the energy balance equation

$$\rho_d \frac{4}{3} \pi r^3 c_d \frac{dT_d}{dt} - \rho_d 4\pi r^2 \frac{dr}{dt} L(T_d) = 4\pi r^2 Q_d \quad (6)$$

Droplet drag coefficient

In compressible flows, the drag coefficient of the rigid sphere C_{DS} was calculated based on the local relative Mach number, $M^{[6]}$.

$$T_r = T_d/T_g \quad S_r = M\sqrt{\gamma/2} \quad Re = 2\rho|\bar{u} - \bar{v}_p|r/\mu$$

Subsonic Regime:

$$t_1 = Re + S_r \left\{ 4.33 + \frac{3.65 - 1.53T_r}{1 + 0.353T_r} e^{\left(-0.247\frac{Re}{S_r}\right)} \right\}$$

$$t_{21} = 0.03 Re + 0.48\sqrt{Re}$$

$$t_2 = \left\{ \frac{4.5 + 0.38t_{21}}{1 + t_{21}} + 0.1M^2 + 0.2M^8 \right\} e^{\left(\frac{-M}{2\sqrt{Re}}\right)}$$

$$t_3 = 0.6S_r \left(1 - e^{\frac{-M}{Re}} \right)$$

$$C_{DS} = 24/t_1 + t_2 + t_3$$

Supersonic Regime:

$$t_1 = 1.86\sqrt{M/Re}$$

$$t_2 = 0.9 + t_1 \left(2 + \frac{2}{S_r^2} + \frac{1.058\sqrt{T_r}}{S_r} - \frac{1}{S_r^4} \right)$$

$$C_{DS} = t_2/(1 + t_1) \quad (7)$$

However, the drops undergo significant flattening and no longer spherical due to the dynamic pressure effect as soon as they enter the air flow. Correspondingly, the drag coefficient of a distorting drop should be a function of distortion parameter and lie between that of a rigid sphere and that of a disk. It was found that the drag coefficient of sphere in a compressible flow is about 1 and is approximate 1.5 for rigid disk^[7]. By using the distortion parameter γ in the TAB model, a simple expression was proposed based on the method in Ref (8).

$$C_D = C_{DS}(1 + 0.5\gamma) \quad (8)$$

Furthermore, the frontal area of the drop exposed to the flow is also changed due to its distortion, which is expressed below.

$$A_f = \pi r^2 * (1 + \gamma/2)^2 \quad (9)$$

Droplet collision and coalescence

Drop collisions are calculated by a sampling procedure based on the viewpoint of the stochastic particle method. The basic assumptions are that the number of droplets associated with each drop particle is distributed in the computational cell, and the collision calculation is performed for the pair of particles only if they are in the same computational cell. The collision frequency can be calculated, and then be used to solve the probability that a droplet will undergo a collision with a drop in the other particles.

Numerical Technique

The solution procedure was based on a finite volume method called arbitrary Lagrangian-Eulerian (ALE) method. In the Lagrangian phase, the mesh

vertices move with the gas velocity, and there is no convection across cell boundaries. Spray droplet collision, evaporation and breakup terms are calculated. Meanwhile, mass and energy source terms due to spray are treated by explicit scheme. Implicit differencing is then used for all the diffusion terms and the terms associated with pressure wave propagation of the gas equations as well as the spray momentum source term. The coupled implicit equations are solved by a method similar to the SIMPLE algorithm, with individual equation being solved by the conjugate residual method. In the rezone phase, the flow field is frozen and remapped onto new computational mesh. Explicit methods are used to calculate convection, which is subcycled several times due to the restriction of Courant stability condition.

Surrogate Model of Kerosene

Liquid hydrocarbon fuels are complex mixtures of many components. A surrogate fuel model composed of a neat compound or several neat components has to be developed for computational efficiency reason, while important thermo-physical properties are retained. In present work, the surrogate fuel model $C_{12}H_{24}$ was proposed as a generic representation for kerosene^[9].

Boundary Conditions

All the parameters at the entrance of computational domain were given. The combustor wall was considered to be adiabatic and a wall function was employed. The value of y^+ at the first point from the wall is less than 60. The flow variables at outflow boundaries were determined by 1st-order extrapolation from the computational domain.

The dispersed phase may be introduced anywhere within the flow domain, at which droplet mass flow rate and distribution of droplet sizes, velocity, temperature, cone angle and oscillation parameters were specified.

χ -squared distribution was used for the sizes of injected droplets. The cone angle of the spray was specified as 30° . The kerosene is room temperature. The velocities of the drops all have same magnitude calculated via the fuel injection pressure.

3 Results and Discussions

Simulation was conducted to study the kerosene spray injecting through the wall orifice into the Mach 2.5 cross flow with the static temperature of 430K and static pressure of 0.043MPa. Fuel injection pressure was 2.2MPa, and the orifice diameter was 0.8mm. Additionally, the verification of numerical simulation was carried out by experimental Schlieren image.

Analysis and Comparison with Schlieren Image

In the calculation, the initial Sauter Mean Radius (SMR) of the drops was given $35\mu\text{m}$ based on the measurement at the 70mm downstream of the injecting orifice by Particle Dynamics Analyzer in case of

kerosene injecting into quiescent atmosphere.

Fig.1(a) and (b) demonstrate the numerical spray structure and pressure contour. In Fig.1(a), the color denotes the droplet size. It is found that a bow shock wave appears upstream of the injector due to the obstruction of the liquid jet. Meanwhile, Spray is severely bent by the gas flow. Smaller droplets have lower inertia and more quickly follow with the gas flow, thus larger droplets are at the periphery of spray. Furthermore, the crimped spray plume reveals the influence of the turbulent diffusion.

The corresponding visualization images of the kerosene spray in supersonic combustor taken by schlieren were shown in Fig.1(c). Through the comparison, the numerical and experimental kerosene spray plumes showed good agreement.

Fig.2 further quantitatively shows the variation of the average SMR of droplets at the cross section with axial location. It is clear that initial parent drops are broken up into small drops whose diameter is about $O(10)$ micrometers soon after they enter into the supersonic cross flow. It may be attributed to the effect of secondary breakup. Because the Weber number of the droplet issued from the injector into the supersonic cross flow is over 1000, then the so-call 'catastrophic' breakup phenomenon will occur^[10].

Pilch had deeply investigated the breakup of a liquid drop in the gas flow^[11]. Total breakup time for low-viscosity drops are given by:

$$t_{bu} = T\sqrt{\rho_d/\rho} 2r/V, \quad (10)$$

Here, T is a dimensionless time characteristic of drop breakup by Rayleigh-Taylor or Kelvin-Helmholtz instability.

$$T = 0.766(We - 12)^{0.25}, \quad 351 < We < 2670$$

$$T = 5.5, \quad We \geq 2670 \quad (11)$$

For this simulation case, the Weber number of the initial droplets is about 1000~2000, then T can be calculated to be between 4.3 and 5.5, while the breakup time should be about $O(10^{-5})\text{s}$.

Pilch had also recommended the following empirical correlation of drop displacement in its breakup process:

$$\frac{x}{2r} = \frac{3}{8}C_d T^2 + BT^3 \quad (12)$$

For compressible flow, $C_d=1$, $B=0.116$

When the breakup process ceases, the drop axial displacement can be derived to be:

$$x \cong 50r \quad (13)$$

For droplets with the radius of $35\mu\text{m}$, the aerodynamic secondary breakup process is complete at

1.75mm downstream of the injector, which verifies the numerical results: initial parent drops are broken up into small drops whose diameter is about O(10) micrometers soon after they enter into the supersonic cross flow.

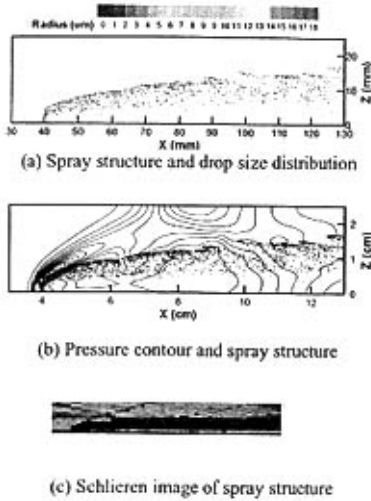


Fig.1 Numerical and experimental kerosene spray
 $P_f=2.2\text{MPa}$ $d_o=0.8\text{mm}$

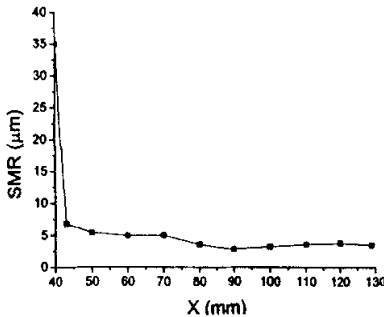


Fig.2 Variation of average SMR of droplets at the cross section with axial location

Effect of the Initial Drops Size on secondary breakup

In order to further study the secondary breakup effect of the supersonic cross flow on the initial parent droplets, the cases with different initial droplet sizes were investigated, while other conditions were the same as above case.

Fig.3 demonstrates the spray structures with three different initial drops SMR, 35µm, 60µm and 100µm respectively. Fig.4 further shows the quantitative comparison of average spray parameter for three cases,

including droplets SMR, velocity, and temperature. From Fig.3 and Fig.4(a), it can be found that drop size and penetration of the spray are insensitive to initial drop SMR.

Based on Ref(11), the breakup is envisioned as a multistage process in which fragments will be subject to further breakup as long as the fragments have Weber number exceeding the critical value. When the multistage process is complete, all the fragments will smaller than a critical size — the maximum stable diameter.

A fragment whose Weber number equals the critical Weber number has a diameter equal to the maximum stable diameter. An estimate of the maximum stable diameter was given by^[11]:

$$d_{stable} = We_{cr} \frac{\sigma}{\rho V_d^2} \left(1 - \frac{V_d}{V_r}\right)^{-2} \quad (14)$$

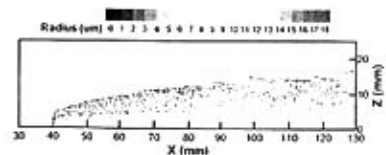
Here, V_d is the velocity of the fragment cloud when all breakup processes cease.

$$\frac{V_d}{V_r} = \sqrt{\frac{\rho}{\rho_d} \left(\frac{3}{4} C_d T + 3BT^2\right)} \quad (15)$$

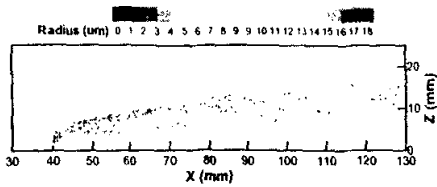
From Eq.(11), the dimensionless time T is from 4.3 to 5.5. Then it can be derived through Eq.(14) and (15) that the maximum stable drop diameters with different initial drop size are nearly same magnitude with their relative difference less than 20%.

Combined with Eq.(13), at 50r downstream of the injector (during the appropriate range of initial drop size, it is less than 5mm), droplets with different size will be broken up into small drops with the same magnitude diameter. In summary, the numerical simulation agree with the pilch's experimental and analytical results

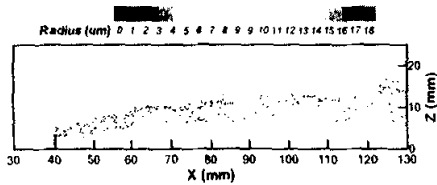
So it can be concluded that, during the appropriate range of initial drop size, the parent droplets will be instantaneously broken up into small drops with the same magnitude diameter no matter how large the initial drops SMD is. Subsequently, the small drops would almost move in the same manner. As shown in Fig.4(b)-(d), the small drops with different initial drop size have the same variation in the drops temperature and drops velocity. It is further demonstrated in Fig.3 that three kerosene spray plumes have nearly the same penetration.



(a) $P_f=2.2\text{MPa}$ $d_o=0.8\text{mm}$ Initial SMR of 35µm

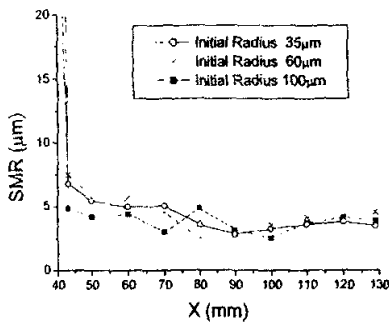


(b) $P_f=2.2\text{MPa}$ $d_0=0.8\text{mm}$ Initial SMR of $60\mu\text{m}$

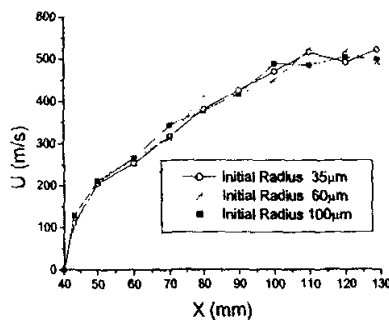


(c) $P_f=2.2\text{MPa}$ $d_0=0.8\text{mm}$ Initial SMR of $100\mu\text{m}$

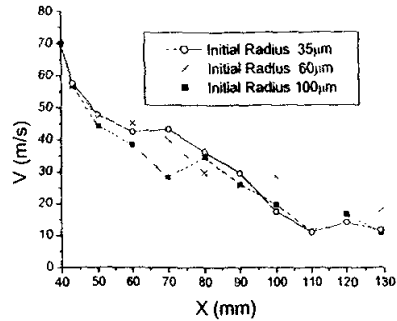
Fig.3 Spray structure and drop size distribution with different initial drop SMR



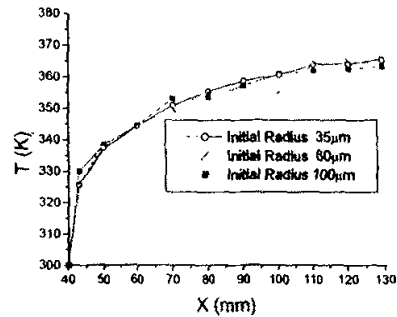
(a) Variation of SMR of droplets



(b) Variation of axial velocity of droplets



(c) Variation of transverse velocity of droplets



(d) Variation of droplets temperature

Fig.4 Variation of average spray parameter at the cross section with axial location

4 Conclusions

Numerical simulation was conducted to study the kerosene spray characteristics injecting into supersonic cross flow. A stochastic particle method is used to calculate the liquid sprays, in which various sub-models account for the effects of turbulent dispersion, droplet collisions, evaporation and aerodynamic breakup. The corresponding visualization images of the kerosene spray in supersonic combustor were also taken by schlieren to verify the numerical results. It was found that:

1. A bow shock wave was captured upstream of the injector when spray was injected into supersonic cross flow. Meanwhile, Spray is severely bent by the gas flow.
2. During the appropriate range of initial drop size, the parent droplets will be instantaneously broken up into small drops with the same magnitude diameter $O(10)$ micrometers no matter how large the initial drops SMD is. Then the small drops move almost in the same manner.
3. The numerical and experimental kerosene spray plumes showed good agreement.

5 Acknowledgement

Current research program was supported by the National Science Foundation of China 10102022.

6 References

1. G.Yu, J.G.Li, X.Y.Zhang, L.H.Chen, C.J.Sung, "Investigation of Kerosene Combustion Characteristics with Pilot Hydrogen in Model Supersonic Combustors", Journal of Propulsion and Power, Vol.17, No.6, Nov.-Dec., 2001.
2. Yue Lianjie, Yu Gong, "Numerical Simulation of Kerosene Spray in Supersonic Cross Flow", Journal of Propulsion Technology, Vol.25, No.1. (In Chinese)
3. A.A.Amsden, P.J.O'Rourke, and T. D. Butler, "KIVA-II: A Computer Program for Chemically Reactive Flows with Sprays," Los Alamos National Laboratory report LA-11560-MS (May 1989).
4. R.D.Reitz, C.J.Rutland, "Development and Testing of Diesel Engine CFD Models", Prog. Energy Combust. Sci., Vol.21, pp.173-196, 1995.
5. P.J.O'Rourke, A.A.Amsden, "the TAB method for numerical calculation of spray droplet breakup", SAE 872089
6. "CFD-ACE Theory Manual"
7. P.G.Simpkins, E.L.Bales, "Water-Drop Response to Sudden Accelerations", J. Fluid Mech., Vol.55, Part4, pp.629-639, 1972.
8. Alex B.Liu, Daniel Mather, Rolf D.Reitz, "Modeling the effects of Drop Drag and Breakup on Fuel Sprays", SAE 930072.
9. T.-S.Wang, "Thermophysics Characterization of Kerosene Combustion", AIAA 2000-2511
10. C.H.Lee, Rolf D.Reitz, "An Experimental Study of the Effect of Gas Density on the Distortion and Breakup Mechanism of Drops in High Speed Gas Stream", International Journal of Multiphase Flow, 26 (2000), pp.229-244.
11. M.Pilch, C.A.Erdman, "Use of Breakup Time Data and Velocity History Data to Predict the Maximum Size of Stable Fragments for Acceleration-Induced Breakup of a Liquid Drop", International Journal of Multiphase Flow, Vol.13, No.6, pp.741-757, 1987.

7 Nomenclature

c_d	Liquid specific heat
C_D	Aerodynamic drag coefficient of liquid drop
C_{DS}	Drag coefficient of rigid sphere
D	Diffusion coefficient
d_{stable}	Maximum stable diameter of drop
\bar{g}	Gravitational acceleration
$L(T_d)$	Latent heat of vaporization
Q_d	Rate of the heat conduction to the drop surface per unit area
r	Droplet radius

We	Weber number
s_{ij}	Mean stress rate tensor
Sh_d	Sherwood number for mass transfer
t_{ba}	Drop breakup time
T	Dimensionless time of drop breakup
T_d	Droplet temperature
\bar{u}	Fluid velocity
\bar{u}'	Gas turbulence velocity
\bar{v}_p	Droplet velocity
V_r	Initial relative velocity between gas and drop the axial displacement of droplets
x	Kerosene vapor mass fraction at droplet's surface
Y_l^*	Distortion parameter of drop surface oscillation
y	Gas density
ρ	Liquid density
ρ_d	Turbulence kinetic energy
k	Turbulence kinetic energy dissipation
ε	Gas viscosity
μ	Viscosity of the liquid fuel
μ_l	Surface tension
σ	